The orexin OX1 receptor exists predominantly as a homo-dimer in the basal state: Potential regulation of receptor organisation by both agonist and antagonist ligands

Tian-Rui Xu, Richard John Ward, John D. Pediani, Graeme Milligan

The orexin OX_1 receptor exists predominantly as a homo-dimer in the basal state: Potential regulation of receptor organisation by both agonist and antagonist ligands

Tian-Rui Xu*, Richard J. Ward*, John D. Pediani and Graeme Milligan[1]

*these authors contributed equally to the work

Molecular Pharmacology Group, Institute of Neuroscience and Psychology, College of Medical, Veterinary and Life Sciences, University of Glasgow, Glasgow G12 8QQ, Scotland, U.K.

[1]Corresponding author:

Graeme Milligan, 253 Wolfson Link Building, University of Glasgow, University Avenue, Glasgow G12 8QQ, Scotland, UK
Tel: +44 141 330 5557, FAX: +44 141 330 5481,
e-mail: Graeme.Milligan@glagow.ac.uk

Short title: The orexin OX_1 receptor exists as a homo-dimer

SYNOPSIS

It is unclear what proportion of a G protein-coupled receptor is present in cells as dimers or oligomers. Saturation BRET studies demonstrated the orexin OX_1 receptor to be present in such complexes. Forms of this receptor containing a minimal epitope tag, with the C-terminus linked to YFP or modified at the N-terminus to incorporate a SNAP-tag, migrated in SDS-PAGE as monomers indicating a lack of covalent interactions. Solubilisation with dodecylmaltoside, followed by Blue Native-PAGE, indicated the receptor constructs migrated predominantly as anticipated for dimeric species with evidence for further, higher-order complexes and this was true over a wide range of expression levels. Addition of SDS prior to separation on Blue Native-PAGE resulted in much of the previously dimeric, and all of the higher-order, complexes being dissociated and now migrating at the size predicted for monomeric species. Expression of forms of the OX_1 receptor capable of generating enzyme complementation confirmed that solubilisation *per se* did not result in interaction artefacts. Addition of the endogenous agonist orexin A enhanced the proportion of higher-order OX_1 receptor complexes whilst selective OX_1 antagonists increased the proportion the OX_1 receptor migrating in Blue Native-PAGE as a monomer. The antagonist effects were produced in a concentration-dependent manner, consistent with the affinity of the ligands for the receptor. Homogeneous time-resolved FRET studies using Tag-Lite™ reagents on cells expressing the SNAP-tagged OX_1 receptor identified cell surface OX_1 homomers. Predominantly at low receptor expression levels orexin A increased such FRET signals, also consistent with ligand-induced re-organization of the homomeric complex.

Key words: Blue Native-PAGE, homo-dimer, orexin OX_1 receptor, receptor organisation.

Abbreviations used: BN-PAGE, Blue Native-polyacrylamide gel electrophoresis; BRET, Bioluminescence resonance energy transfer; DDM, *n*-dodecyl-β-D-maltoside; EGF, Epidermal growth factor; FRAP, fluorescence recovery after photobleaching; GPCR, G protein-coupled receptor; htrFRET, homogenous time resolved FRET; SDS-PAGE, sodium dodecyl sulphate-polyacrylamide gel electrophoresis.

Chemical names:
SB334867; N-(2-methyl-6-benzoxazolyl)-N'-1,5-naphthyridin-4-yl urea SB408124; N-(6,8-Difluoro-2-methyl-4-quinolinyl)-N'-[4-(dimethylamino)phenyl]urea SB674042; 1-(5-(2-fluoro-phenyl)-2-methyl-thiazol-4-yl)-1-((*S*)-2-(5-phenyl-(1,3,4)oxadiazol-2-ylmethyl)-pyrrolidin-1-yl)-methanone

INTRODUCTION

In recent years the concept that G protein-coupled receptors (GPCRs) exist in cells exclusively as independent, non-interacting monomeric species [1] has largely been overtaken by a view that they can exist as dimeric, or even oligomeric, complexes [2-3]. However, apart from members of the class C, metabotropic glutamate-like receptors that exist as obligate homomers or heteromers [4] and where disulphide bonds between the large, extracellular Venus flytrap-like domains act to partially stabilise the multi-protein complex, there is little evidence to indicate that receptor dimers/oligomers are linked covalently. This implies that for the large family of class A, rhodopsin-related GPCRs, the extent of dimeric or oligomeric assembly must be related to the interaction affinities between individual GPCR protomers. This may potentially vary significantly between individual GPCRs, particularly if, as has been suggested in a number of studies [3], different transmembrane elements contribute to interactions between individual GPCRs. Despite this, relatively little is known about the dynamics and regulation of GPCR oligomer formation and/or stability and even less is known about the proportion of individual GPCRs that is present as dimers/oligomers. However, there is some direct evidence to suggest differences in affinity of such interactions between even closely related GPCRs. For example, using fluorescence recovery after photobleaching (FRAP) techniques it was demonstrated that whilst the β_2-adrenoceptor appears to form a stable oligomeric complex, parallel studies on the β_1-adrenoceptor suggested it to form a more transient complex [5]. Equally, by employing total internal reflectance fluorescence microscopy Hern and co-workers have shown that dimers of the muscarinic M_1 receptor appear to associate and dissociate on the time scale of seconds [6].

The orexin receptors OX_1 and OX_2 are members of the rhodopsin-like family of GPCRs [7]. Ligand pairing of these receptors with the peptides orexin A and orexin B, both derived from the precursor prepro-orexin [7], instigated a wide range of studies on their biological function that have centred on the regulation of sleep/wakefulness and in the control of feeding and appetite [8,9]. Based on such studies agonism of orexin receptors has been suggested as a means to treat narcolepsy whilst orexin receptor antagonists have been promoted as a potential treatment of sleep disorders such as insomnia. Indeed, the combined OX_1 and OX_2 antagonist almorexant has undergone late stage clinical trials in this area [10]. In previous studies we have shown that when expressed from an inducible promoter in Flp-In™ T-REx™ 293 cells, modified forms of the human OX_1 receptor migrate on sodium dodecyl sulphate-polyacrylamide gel electrophoresis (SDS-PAGE) as apparently single polypeptides [11]. This is in contrast to a number of other class A GPCRs that show complex migration patterns, often associated with differential N-glycosylation. In the current studies we use the human OX_1 receptor to explore the propensity of this GPCR to form homo-dimers/oligomers and, via Blue Native-PAGE (BN-PAGE) [12,13] demonstrate that at a range of expression levels the OX_1 receptor exists predominantly as a homo-dimer in the basal state. This is the first study to define the proportion of a GPCR present in cells as a homo-dimer. We also use combinations of cell surface, homogenous time-resolved (htr) FRET [14,15] and Blue Native-PAGE to explore if ligand binding to the OX_1 receptor alters receptor quaternary organisation and an enzyme complementation strategy [16] based on a split *Renilla* luciferase variant [17] to ensure that membrane receptor solubilisation by *n*-dodecyl-β-D-

maltoside (DDM) prior to Blue Native-PAGE does not inherently produce OX_1 receptor interaction artefacts.

EXPERIMENTAL

Materials

[^{3}H]SB-674042 (1-(5-(2-fluoro-phenyl)-2-methyl-thiazol-4-yl)-1-((*S*)-2-(5-phenyl-(1,3,4)oxadiazol-2-ylmethyl)-pyrrolidin-1-yl)-methanone) was from GE Healthcare (Amersham, UK). Orexin A was a gift of GlaxoSmithKline (Harlow, U.K.) or from Bachem UK Ltd, (St Helens, Merseyside, U.K.). *Renilla* luciferase 8 (Rluc8) [17] cDNA was a gift of Dr. S.S. Gambhir, Stanford University School of Medicine, CA. SB-334867 (N-(2-methyl-6-benzoxazolyl)-N'-1,5-naphthyridin-4-yl urea) and SB-408124 (N-(6,8-Difluoro-2-methyl-4-quinolinyl)-N'-[4-(dimethylamino)phenyl]urea) were from Tocris Biosciences, (Avonmouth, UK). Polyclonal rabbit epidermal growth factor (EGF) receptor antibody and rabbit anti-HA were from Santa Cruz (Insight Biotechnology, Wembley, UK). Polyclonal rabbit anti-VSV-G antiserum was generated in house. Flp-In™ T-REx™ 293 cells and Lipofectamine 2000 transfection reagent were from Invitrogen, (Paisley, UK). Protease inhibitor cocktail tablets were from Roche Diagnostics (Mannheim, Germany). Monoclonal mouse anti-VSV-G antibody and all other materials were supplied by Sigma Aldrich Company Ltd (Poole, UK) or Fisher Scientific (Loughborough, UK).

DNA constructs

The plasmids for expression of the constructs VSV-G-OX_1-eYFP and VSV-G-SNAP-OX_1 were generated as described by [11] and [18] respectively. PcDNA3.1-VSV-G-OX_1-Rluc8 was generated by replacing the eYFP of pcDNA3.1-VSV-G-OX_1-eYFP with Rluc8. The primers were CGA TCG ATG CGG CCG CCA TGG CTT CCA AGG TGT ACG ACC C (forward with NotI site) and TCG TCT CGA GTT ACT GCT CGT T CT TCA GCA CGC GCT (reverse with XhoI site). PcDNA3.1-VSV-OX_1-Rluc8 N-terminal split (amino acids 1-229) and pcDNA3.1-VSV-G-OX_1-Rluc8 C-terminal split (amino acids 230-311) were generated by the same strategy. The primers for the Rluc8 N-terminal split were CGA TCG ATG CGG CCG CCA TGG CTT CCA AGG TGT ACG ACC C (forward with NotI site) and TCG TCT CGA GTT AGC CTCC CTT AAC GAG AGG GAT CTC (reverse with XhoI site). The primers for the Rluc8 C-terminal split were CGA TCG ATG CGG CCG CCAA GCC CGA CGT CGT CCA GAT TGT (forward with NotI site) and TCG TCT CGA GTT ACT GCT CGT T CT TCA GCA CGC GCT (reverse with XhoI site). PcDNA3-FLAG-α_{1b}-adrenoceptor-eYFP was constructed as described [19], pcDNA3-FLAG-α_{1b}-adrenoceptor-Rluc8 was generated by replacing the eYFP of pcDNA3-FLAG-α_{1b}-adrenoceptor-eYFP with Rluc8. The primers were CGA TGG TAC CAT GGC TTC CAA GGT GTA CGA CCC (forward with KpnI site) and TCG TGC GGC CGC TTA CTG CTC GTT CTT CAG CAC GCG CT (reverse with NotI site). To generate a minimally tagged form of the OX_1 receptor, a stop codon was added to the end of the OX_1 sequence of the pcDNA5/FRT/TO VSV-G-OX_1-eYFP construct. The primers used were GTC ACC ACA GTG CTG CCC TGA GCC GCC GTG AGC AAG GG (forward) and CCC TTG CTC ACG GCG GCT CAG GGC AGC ACT GTG GTG AC (reverse).

Generation and maintenance of stable Flp-In™ T-REx™ 293 cells

To generate Flp-In™ T-REx™ 293 cells able to inducibly express the VSV-G-OX_1, VSV-G-OX_1-eYFP [11] or VSV-G-SNAP-OX_1 [18] constructs cells were co-transfected with the plasmid pOG44 and the desired cDNA in pcDNA5/FRT/TO (Invitrogen) at a ratio of 9:1 using Lipofectamine. After 48 h the medium was supplemented with 200 $\mu g.ml^{-1}$ hygromycin to select for stably transfected cells. Pools of cells were established and tested for inducible expression by the addition of 1 $\mu g.ml^{-1}$ doxycycline for 48 h followed by screening for VSV-G or SNAP-tag protein expression by Western blotting. A further cell line was established using the VSV-G-OX_1-eYFP inducible Flp-In™ T-REx™ 293 cells as a base. These cells were transfected with pcDNA3.1-HA-OX_1-eYFP [20] and clones resistant to the presence of 1 $mg.ml^{-1}$ G418 were screened initially for the presence of eYFP in the absence of doxycycline (as VSV-G-OX_1-eYFP is not expressed in this situation) and subsequently to detect anti-HA immunoreactivity.

Co-immunoprecipitation studies

The cells described above were untreated or VSV-G-OX_1-eYFP expression was induced by treatment with doxycycline for 24 h. Cells were harvested and treated with lysis buffer (150 mM NaCl, 0.01 mM Na_3PO_4, 2 mM EDTA, 0.5 % DDM, and 5% glycerol plus protease inhibitor cocktail tablets, pH 7.4) on a rotating wheel for 30 min at 4°C. Samples were then centrifuged for 30 min at 100,000*g* at 4°C, and the supernatant was transferred to a fresh tube and incubated with anti-VSV-G agarose beads (Sigma) for 2 h at 4°C on a rotating wheel. Samples were subsequently washed four times with lysis buffer. The bound receptors were eluted with 0.2 $mg.ml^{-1}$ VSV-G peptide (Sigma) in lysis buffer and the eluates separated on BN-PAGE. Immunoblotting with anti-HA and anti-VSV-G was then performed.

HEK293T cell culture and transfection

HEK293T cells were maintained in Dulbecco's modification of Eagle's medium (DMEM) supplemented with 0.292 $g.liter^{-1}$ L-glutamine, 1% antibiotic mixture and 10% (v/v) newborn calf serum at 37°C in a 5% CO_2 humidified atmosphere. The cells were transfected using Lipofectamine 2000 reagent according to protocols from the supplier.

Cell membrane preparation

Pellets of cells were frozen at -80°C for a minimum of 1 h, thawed and resuspended in ice-cold 10mM Tris, 0.1mM EDTA, pH 7.4 (TE buffer) supplemented with Complete protease inhibitors cocktail (Roche Diagnostics, Mannheim, Germany). Cells were homogenized on ice by 40 strokes of a glass on Teflon homogenizer followed by centrifugation at 1000 x g for 5 min at 4°C to remove unbroken cells and nuclei. The supernatant fraction was removed and passed through a 25-gauge needle 10 times before being transferred to ultracentrifuge tubes and subjected to centrifugation at 50,000 x g for 30 min at 4°C. The resulting pellets were resuspended in ice-cold TE buffer. Protein concentration was assessed and membranes were stored at -80°C until required.

[^{3}H]SB-674042 binding assays

Saturation binding curves were established by the addition of 5 µg of membrane protein to assay buffer (25mM HEPES, 500mM NaCl, and 2.5mM $MgCl_2$, pH 7.4, supplemented with 0.3% bovine serum albumin, BSA) containing up to 12 nM [^{3}H]SB-674042. Non-specific binding was determined in the presence of 30µM SB408124. Reactions were incubated for 90 min at 25^{o}C, and bound ligand was separated from free by vacuum filtration through GF/C filters (Brandel Inc, Gaithersburg, MD). The filters were washed twice with cold 1 x PBS (120mM NaCl, 25mM KCl, 10mM Na_2HPO_4, 3mM KH_2PO_4 pH 7.4) and bound ligand was estimated by liquid scintillation spectrometry.

[^{3}H]SB-674042 binding assays and DDM solubilisation

Flp-In^{TM} T-REx^{TM} 293 cells harbouring VSV-G-OX_1-eYFP were untreated or induced with doxycycline for 24 h. The cells were harvested and lysed as described for cell membrane preparations and the supernatants collected after the low speed spin. 250µg of protein was added to assay buffer (25mM HEPES, 500mM NaCl, and 2.5mM $MgCl_2$, pH 7.4), containing up to 5nM [^{3}H]SB674042. Non-specific binding was determined in the presence of 3µM SB408124. Reactions were incubated for 90 min at 25°C and then divided into two equal aliquots, which were spun at 20000*g* for 15 min at 4°C and the supernatants removed. The first pellets were washed with 400µl assay buffer and then resuspended in 200µl assay buffer for bound ligand to be determined by liquid scintillation spectrometry. The second pellets were resuspended in 100µl assay buffer supplemented with 0.5% DDM and 5% glycerol before being incubated at 4 °C on a rotating wheel for 30 min. These samples were centrifuged at 100,000g for 60 min at 4 °C and 50µl of the supernatant then applied to a Micro Bio-Spin P-6 column (Biorad) to separate bound from free [^{3}H]SB674042. Protein bound [^{3}H]SB674042 eluted from the column was determined by liquid scintillation spectrometry and values corrected to allow for only half the sample being applied to the Micro Bio-Spin column.

Epifluorescence imaging of SNAP-tag proteins in live cells

Cells able to express VSV-G-SNAP-OX_1 were grown on coverslips which had been cleaned with alcohol and treated with 0.1 mg.ml^{-1} poly-D-lysine. SNAP-tag specific dye substrates were diluted in complete DMEM medium from a 1 mM stock solution to give a labelling solution of 5 µM with respect to the SNAP dye substrate. The cell medium was replaced with labelling solution and incubated at 37°C, 5% CO_2 for 30 min. Cells were washed three times with complete DMEM and once with HEPES physiological saline solution (130mM NaCl, 5mM KCl, 1mM $CaCl_2$, 1mM $MgCl_2$, 20mM HEPES, and 10mM D-glucose, pH7.4). Coverslips were then transferred to a microscope chamber where they were imaged using an inverted Nikon TE2000-E microscope (Nikon Instruments, Melville, NY) equipped with a 40x (numerical aperture-1.3) oil-immersion Pan Fluor lens and a cooled digital photometrics Cool Snap-HQ charge-coupled device camera (Roper Scientific, Trenton, NJ).

Homogeneous time-resolved (htr) FRET studies

Cells induced to express VSV-G-SNAP-OX_1 were seeded at 100000 cells per well in solid black 96 well plates (Greiner BioOne) which had been treated with 0.1 $mg.ml^{-1}$ poly-D-lysine. The growth medium was replaced with 100µl of a mix containing the fixed optimal concentrations of donor (Tag-lite SNAP-Lumi4-Tb) and acceptor (Tag-lite SNAP-Red) in 1 x labelling medium (all from Cisbio Bioassays, Bagnols-sur-Cèze, France). Plates were incubated for 1 h at 37°C, 5% CO_2 in a humidified atmosphere, and subsequently washed four times in labelling medium. Plates were either read directly after this or were subjected to ligand treatment first. For this, appropriate drug concentrations were added to the plates after the last labelling medium wash; they were then incubated at 37°C for the required time and analysed using a PHERAstar FS htrf compatible reader (BMG Labtechnologies, Offenburg, Germany). The emission signal from the Tag-lite SNAP-Lumi4-Tb cryptate (620 nm) and FRET signal resulting from the acceptor Tag-lite SNAP-Red (665 nm) were recorded. The specific htrFRET signal was calculated by subtracting the 665 nm signal obtained from un-induced cells (that is not expressing the receptor), but which had been labelled, from the 665 nm signal of cells expressing the receptor. This, corrected, 665 nm value was then used to calculate the 665/620 FRET ratio.

Blue Native-PAGE and SDS-PAGE

Flp-In™ T-REx™ 293 cells induced with doxycycline to express VSV-G-OX_1-eYFP or VSV-G-SNAP-OX_1 were harvested in PBS and lysed in lysis buffer (150 mM NaCl, 0.01 mM Na_3PO_4, 2 mM EDTA, 0.5 % DDM, and 5% glycerol plus protease inhibitor cocktail tablets, pH 7.4) on a rotating wheel for 30 min at 4°C. Samples were then centrifuged for up to 60 min at 100,000*g* at 4°C, and the supernatants were collected. 18 µg of solubilised supernatant plus 4µl G250 additive (Invitrogen) was loaded on to each lane of NativePAGE™ Novex® 3–12% Bis-Tris Gels (Invitrogen). In certain experiments varying concentrations of SDS were added prior to this stage. After migration at room temperature (24°C), proteins were transferred (90 min at 25 V) on to a PVDF membrane which had been pre-wetted for 30 sec in methanol. The membrane was then fixed in 8% acetic acid for 15 min and immunoblotted with anti VSV-G antibody or anti VSV-G antiserum. For SDS-PAGE, the same set of solubilised supernatants were mixed with 2 x SDS loading buffer and after heating to 65°C for 15 min, samples were resolved on 4-12% NuPAGE Bis-Tris Gels (Invitrogen) and subsequently immunoblotted to detect proteins of interest.

BRET assays

HEK293T cells were co-transfected with receptor-Rluc8 and receptor-eYFP constructs in 6 well plates, 24 h post-transfection, cells were trypsinized and transferred to poly-D-lysine coated, white wall 96-well plates (for BRET and luminescence reading) and black wall 96-well plates (for eYFP reading). 48 h post-transfection, cells in black well 96-well plates were washed with HBSS (Invitrogen) and the expression of eYFP was measured on a PHERAstar FS (BMG Labtechnologies). Cells in white wall 96-well plates were washed and incubated in HBSS at 37°C for 30 min, then coelenterazine-h was added (5 µM final concentration) and incubated for another 10 min in the dark at 37°C, BRET was measured on a PHERAstar FS. For BRET saturation assays, cells were co-transfected

with a fixed amount of the Rluc8-tagged receptor construct and increasing amounts of the eYFP-tagged receptor construct. Net BRET signal was plotted as a function of eYFP (energy acceptor) divided by Rluc8 (energy donor) fusion expression (eYFP/Rluc8). The curves were fit using a non-linear regression equation assuming a single binding site with Prism v5.0. The hetero-titration curve of OX_1-Rluc8/α_{1b}-adrenoceptor-eYFP was achieved by transfecting a fixed amount of OX_1-Rluc8 (0.5 µg/well) and increasing amounts of α_{1b}-adrenoceptor-eYFP. The hetero-titration curve of α_{1b}-adrenoceptor-Rluc8/OX_1-eYFP was achieved in a similar manner.

Enzyme complementation assay of solubilised receptors

HEK293T cells were transfected with OX_1-Rluc8 N-terminal split or OX_1 receptor-Rluc8 C-terminal split respectively, or co-transfected with both forms. Transfected cells were solubilised in lysis buffer (150 mM NaCl, 0.01 mM Na_3PO_4, 2 mM EDTA, 0.5 % DDM, and 5% glycerol plus protease inhibitor cocktail tablets, pH 7.4). Samples were then centrifuged for 15 min at 15,000*g* at 4°C, and supernatants were collected. 100 µg supernatant (45µl) from mixed single transfections or co-transfections were added into 45 µl HBSS in a white wall 96 well plate. Rluc8 activity was measured by adding 10 µl of 50 µM coelenterazine-h, and reading on a PHERAStar FS.

RESULTS

Flp-In™ T-REx™ 293 cells harbouring a VSV-G-human OX_1 receptor-eYFP (VSV-G-OX_1-eYFP) construct at the Flp-In™ locus [11] were induced to express this polypeptide by treatment with doxycycline for either 22 or 36 h. Imaging the distribution of the eYFP tag in such cells indicated that a high proportion of the induced receptor was present at the cell surface (**Supplementary Figure 1A**). Lysates of these samples were resolved by SDS-PAGE and immunoblotted with anti-VSV-G. As anticipated from previous studies [11], although no VSV-G immunoreactivity was detected without pre-treatment with doxycycline, an apparently single polypeptide of Mr ~90 kDa was present following doxycyline treatment (**Supplementary Figure 1B**). Although this is consistent with detection of a single, monomeric form of this OX_1 receptor construct with limited micro-heterogeneity of N-linked glycosylation or other related modifications, such studies cannot interrogate the potential quaternary organization of the receptor in the cell membrane. To address this, VSV-G-OX_1-eYFP was co-transfected into HEK293T cells with a form of the VSV-G-OX_1 receptor C-terminally tagged with the *Renilla* luciferase variant Rluc8 [18] (VSV-G-OX_1-Rluc8). Bioluminescence resonance energy transfer (BRET) was measured after addition of coelenterazine-h, (**Figure 1**). Co-transfection of VSV-G-OX_1-Rluc8 and VSV-G-OX_1-eYFP in various ratios, followed by addition of coelenterazine-h, resulted in BRET signals that increased over a range of low energy acceptor to energy donor ratios but subsequently reached a maximal level and saturated at higher energy acceptor to energy donor ratios (**Figure 1A**). Such studies are consistent with at least a proportion of the OX_1 receptors forming dimeric or oligomeric complexes [21]. Substantially lower BRET signals were produced at the same eYFP (energy acceptor) to Rluc8 (energy donor) ratio when VSV-G-OX_1-Rluc8 was co-transfected with α_{1b}-adrenoceptor-eYFP or when the energy acceptor/energy donor configuration was

reversed by co-transfection of VSV-G-OX_1-eYFP and α_{1b}-adrenoceptor-Rluc8 (**Figure 1B**).

To attempt to explore the proportion of OX_1 receptors that exist in such complexes we initially assessed the fraction of OX_1 receptors that could be solubilised by treatment with the detergent DDM. Lysates from both uninduced cells and those induced to express VSV-G-OX_1-eYFP were treated with the OX_1 receptor antagonist [^{3}H]SB-674042 (5 nM) in the absence and presence of a second, unlabelled OX_1 receptor antagonist, SB-408124 (3 μM) to define non-specific binding. Although no specific binding of [^{3}H]SB-674042 was detected without treatment of the cells with doxycycline (**Figure 2**), 3.7 +/- 0.08 pmol.mg protein^{-1} of specific [^{3}H]SB-674042 binding was present after induction (**Figure 2**). Such lysates were subjected to treatment with 0.5% DDM. Following sustained centrifugation (100,000 *g* for 1h at 4°C) the non-solubilised material was resuspended and the presence of specific [^{3}H]SB-674042 binding sites assessed. Recovery in this fraction was 24.7% of the specific [^{3}H]SB-674042 binding of the lysate, indicating that approximately 75% of the OX_1 receptor construct was solubilised or unfolded by this treatment. Specific binding of [^{3}H]SB-674042 was also assessed in the solubilised fraction and recovered after passage through a Micro Bio-Spin P-6 column. 75.8 +/- 1.0 % of the specific binding sites potentially solubilised by treatment with DDM (and therefore 57.1% of the binding sites in the initial lysate) were recovered by this process (**Figure 2**) indicating the stability of VSV-G-OX_1-eYFP in 0.5% DDM. Subsequently, cell lysates from non-induced Flp-In™ T-REx™ 293 cells and those induced to express VSV-G-OX_1-eYFP for either 22 or 36 h were treated with 0.5% DDM in the same way and following sustained centrifugation the material in the supernatant was subsequently resolved by Blue Native-PAGE (BN-PAGE) after addition of G250. In such gels the vast majority of the induced anti-VSV-G immunoreactivity migrated with mobility corresponding to reference proteins of some 180 kDa, potentially consistent with a dimeric form of VSV-G-OX_1-eYFP (**Figure 3A**). Indeed, sustained exposure of such immunoblots was required to observe a small proportion of an apparent 90 kDa species (**Figure 3A**) and, at this level of exposure, a series of apparent higher-order species could also be detected (**Figure 3A**). There are potential issues with the use of BN-PAGE to assess the molecular mass and organisation of solubilised transmembrane proteins [22] but addition of SDS to such samples is anticipated to result in their resolution and migration as monomers if the protein is not simply aggregated irreversibly or the migration reflects a monomeric protein still encased in the detergent used for solubilisation [22]. Varying concentrations of SDS were added to samples prior to resolution by BN-PAGE. At concentrations of SDS below 0.1%, no clear differences were noted in mobility of the VSV-G reactive complex. However, at 0.1% SDS there was the appearance of a small degree of immunoreactivity consistent with a monomer and this was greatly increased at 1% SDS (**Figure 3B**). Importantly, migration in BN-PAGE of the epidermal growth factor receptor (175kDa) expressed endogenously by the cells, was at the size anticipated for a monomer and unaffected by the addition of 1% SDS to samples prior to BN-PAGE (**Figure 3C**). Addition of EGF is known to generate a non-covalently associated dimeric complex of the receptor [23,24], and after addition of 100 ng.ml^{-1} EGF for 5 min prior to solubilisation with 0.5% DDM a substantial proportion of the epidermal growth factor receptor now migrated in BN-PAGE with the size anticipated for a dimeric complex **(Figure 3C**) and this was reversed by addition of 1% SDS (**Figure 3C**). To further explore the possibility that the DDM solubilisation resulted in artificial aggregation of the OX_1 receptor, populations of HEK293T cells were

transfected individually with forms of the VSV-G-OX_1 receptor C-terminally tagged with either amino acids 1-229 (Rluc8N) or amino acids 230-311 (Rluc8C) of Rluc8. These fragments are known to be able to complement and generate luciferase activity if they are linked to polypeptides that interact and hence bring the *Renilla* luciferase fragments into proximity [16,17]. Following initial solubilisation with 0.5% DDM the supernatant samples were mixed. However, this process did not result in Rluc8 complementation and luciferase activity (**Figure 4**). By contrast, solubilisation of lysates of HEK293T cells transfected to co-express VSV-G-OX_1-Rluc8N and VSV-G-OX_1-Rluc8C produced a high level of luciferase activity (**Figure 4**), indicating the presence of a dimeric or oligomeric population of the OX_1 receptor in the DDM solubilised fraction derived from the co-transfected cells that was not dissociated by detergent extraction.

The inducible nature of expression from the T-REx™ locus of Flp-In™ T-REx™ 293 cells [11,15,25] allowed different amounts of VSV-G-OX_1-eYFP to be expressed by varying the time of treatment with doxycycline (**Figure 5**). Ligand binding studies employing the OX_1 receptor antagonist [^{3}H]SB674042 allowed measurement of the total number of OX_1 receptor binding sites present at each time point (**Figure 5A**). This indicated that over a 48 h period of induction of VSV-G-OX_1-eYFP, levels of the construct in cell lysates increased from being undetectable up to some 6 pmol.mg protein^{-1}. BN-PAGE was again used to resolve samples from cells induced for varying times that were solubilised using 0.5% DDM and showed that across the full range of expression levels achieved the vast majority of the receptor construct migrated with an apparent mass consistent with a dimer (**Figures 5B, 5C**). As previously, addition of 1% SDS to the samples prior to resolution resulted in a much greater proportion of the immunodetected protein migrating at a position consistent with a monomer (**Figure 5B**). Interestingly, although addition of orexin A (1 x 10^{-6}M or 1 x 10^{-7}M) prior to treatment with DDM had limited effects on the mobility of VSV-G-OX_1-eYFP in BN-PAGE (**Figure 6A**), addition of either of the OX_1 receptor antagonists SB334867 and SB408124 (1 x 10^{-6}M) resulted in a significant proportion of VSV-G-OX_1-eYFP migrating in the position of a monomer in BN-PAGE (**Figure 6A**). This effect of SB334867 was produced in a concentration-dependent manner with pEC_{50} = 7.9 ± 0.17 (**Figures 6B, 6C**), close to the reported binding affinity of this ligand for the OX_1 receptor in preparations of membranes expressing this receptor [18].

The addition of large tags to transmembrane proteins may alter avidity of interaction and/or produce interaction artefacts. In order to exclude the possibility that the eYFP fused to the OX_1 carboxy-terminal was influencing substantially the monomeric/multimeric state of the OX_1 receptor we modified the construct by introduction of a stop codon at the end of the OX_1 sequence. The VSV-G-OX_1 expression construct so produced was also used to generate a Flp-In™ T-REx™ 293 cell line to allow inducible and controlled expression. Following induction these cells were also subjected to ligand treatments and analysis by BN-PAGE (**Figure 7A**). Apart from enhanced mobility consistent with lack of the eYFP tag (**Figure 7A**) VSV-G-OX_1 behaved in a similar manner to VSV-G-OX_1-eYFP. Orexin A had limited effects whilst SB334867 again resulted in a higher proportion of the OX_1 receptor migrating at a position consistent with a monomeric species. Treatment of these cells with various concentrations of SB334867 also resulted in concentration-dependent alteration in the migration pattern of VSV-G-OX_1 to favour the monomer although the ligand appeared to be somewhat less potent (pEC_{50} = 7.33 ± 0.28) at this construct (**Figures 7B, 7C**).

It was at least conceptually possible that the apparent 180kDa form of VSV-G-OX_1-eYFP on BN-PAGE corresponded to the interaction of a monomeric VSV-G-OX_1-eYFP receptor plus a second, undefined protein with similar molecular mass. To assess this we established a further Flp-In™ T-REx™ 293 cell line in which VSV-G-OX_1-eYFP was located at the inducible locus whilst HA-OX_1-eYFP was expressed constitutively (**Figure 8**). In the absence of doxycycline treatment only HA-OX_1-eYFP was detected whilst following induction with doxycycline co-expression of the two forms of the OX_1 receptor was confirmed by immunoblotting of BN-PAGE resolved cell lysates with anti-HA or anti-VSV-G (**Figure 8**). Following extraction with 0.5% DDM and clearance by centrifugation of lysates from doxycycline-treated cells, immunoprecipitation was performed with anti-VSV-G agarose beads. Elution of the beads with the VSV-G peptide was followed by BN-PAGE and immunoblotting of the eluates. Anti-HA immunoreactivity was detected both at an apparent mass of 180kDa and as higher-order species but even with sustained exposure of blots, no protein consistent with a HA-OX_1-eYFP monomer could be detected (**Figure 8A**). However, following addition of 1% SDS prior to resolution on BN-PAGE the majority of the anti-HA immunoreactivity now migrated with an apparent mass of 90 kDa (**Figure 8A**). The presence of HA-OX_1-eYFP migrating at 180kDa following immunoprecipitation with anti-VSV-G from DDM extracts of these cells is consistent with the 180kDa HA-immunoreactive species being an HA-OX_1-eYFP/VSV-G-OX_1-eYFP dimer and that this is largely disassembled by treatment with 1% SDS (**Figure 8A**). In equivalent studies the eluates of the anti-VSV-G immunoprecipitation were also resolved by BN-PAGE and immunoblotted. VSV-G-OX_1-eYFP was detected as both 180 kDa and 90kDa species (**Figure 8B**) and addition of 1% SDS also greatly increased the relative proportion of the 90kDa species (**Figure 8B**).

To explore potential OX_1 receptor dimerisation in a further, distinct cell system and with a different form of the receptor we also generated a version of the OX_1 receptor that was modified at the N-terminus by addition of an N-terminal leader sequence, derived from the metabotropic glutamate 5 receptor, linked in-frame to the VSV-G epitope tag sequence and the 20 kDa SNAP tag protein, that is based on mammalian O^6-alkylguanine-DNA-alkyltransferase [26], to generate VSV-G-SNAP-OX_1. Such SNAP-tagged constructs have recently been shown to be suitable to allow detection of cell surface protein-protein interactions via homogeneous time-resolved (htr)FRET [14,15,26]. Flp-In™ T-REx™ 293 cells harbouring VSV-G-SNAP-OX_1 were also produced and induced with doxycycline. VSV-G-SNAP-OX_1 is predicted to have a slightly lower molecular mass than VSV-G-OX_1-eYFP and indeed, this was noted when lysates from cells induced to express VSV-G-SNAP-OX_1 were resolved by SDS-PAGE alongside those expressing VSV-G-OX_1-eYFP (**Figure 9A**) and, following solubilisation with 0.5% DDM, BN-PAGE (**Figure 9B**). Again, however, a high proportion of VSV-G-SNAP-OX_1 also migrated in a position consistent with a dimeric species (**Figure 9B**). However, when compared to VSV-G-OX_1-eYFP there was evidence for a greater proportion of VSV-G-SNAP-OX_1 migrating as apparent higher-order species (**Figure 9B, 9C**). As for VSV-G-OX_1-eYFP, the mobility of a significant fraction of VSV-G-SNAP-OX_1 was increased to that anticipated for a monomer following addition of 1% SDS prior to BN-PAGE and the potentially higher-order complexes were completely removed by this treatment (**Figure 9C**). However, the effect of 1% SDS on the proportion of the 90kDa species detected was not as marked as for VSV-G-OX_1-eYFP. Whether with relatively limited expression of VSV-G-SNAP-OX_1 induced with a low concentration of doxycycline, or a higher

level of the receptor construct produced by a maximally effective concentration of doxycycline, addition of orexin A resulted in the appearance of much more pronounced levels of an apparently higher-order complex of VSV-G-SNAP-OX_1 (**Figure 10**) and although not possible to detect at low level expression, addition of either SB334867 or SB408124 to cells expressing higher levels of VSV-G-SNAP-OX_1 resulted in a greater proportion of the receptor construct migrating in BN-PAGE at a position consistent with a monomer (**Figure 10**).

Following induction with doxycycline (10ng.ml^{-1}) cell surface VSV-G-SNAP-OX_1 was identified with the cell impermeant dye SNAP 549 (**Supplementary Figure 2A**). Co-addition of a single concentration (10 nM) of SNAP-Lumi4-Tb as potential htrFRET energy donor and varying concentrations of SNAP-Red as a potential htrFRET energy acceptor resulted in a bell-shaped htrFRET signal measured at 665 nm (**Supplementary Figure 2B**), consistent with the detection of cell surface VSV-G-SNAP-OX_1 dimers/oligomers. When using 10 nM SNAP-Lumi4-Tb the optimal concentration of SNAP-Red was some 160 nM (**Supplementary Figure 2B**). At higher concentrations of SNAP-Red, the FRET signal decreased (**Supplementary Figure 2B**). This reflects that in this situation an increasing fraction of cell surface VSV-G-SNAP-OX_1 dimers will likely have bound a molecule of SNAP-Red to each protomer, limiting FRET (**Supplementary Figure 2B**). Optimal FRET is expected to be obtained when the maximal proportion of dimers bind a molecule of SNAP-Lumi4-Tb to one protomer and a molecule of SNAP-Red to the other protomer (**Supplementary Figure 2B**). Indeed, increasing concentrations of SNAP-Red outcompeted and prevented binding of SNAP-Lumi4-Tb as shown by the decline in SNAP-Lumi4-Tb signal at 620 nm that simply reports binding of this reagent (**Supplementary Figure 2B**). In the absence of induction of VSV-G-SNAP-OX_1 no htrFRET signal was produced (**Supplementary Figure 2B, Figure 11A**) but such signals were generated following induction of VSV-G-SNAP-OX_1 (**Figure 11B-D**) with the extent of htrFRET signal dependent upon the extent of induction of the receptor (**Figure 11B-D**). Although the basis and significance of this is uncertain, the basal 665/620 nm htrFRET signal declined slightly over a 60 minute period (**Figure 11**). This was little affected by treatment with a concentration (10^{-6}M) of the OX_1 antagonists SB334867 and SB408124 expected from their measured K_i values to occupy the bulk of the receptor population (**Figure 11**). However, at lower receptor expression levels, the endogenous agonist orexin A produced a substantial increase in 665/620 nm htrFRET signal that was noted at the shortest time period monitored and maintained throughout a 60 min period (**Figure 11**). This is at least consistent with the agonist promoting the formation of higher-order receptor complexes as observed in the BN-PAGE studies (**Figure 10**) or altering the quaternary structure of the dimeric/oligomeric complexes.

DISCUSSION

Although a large number of studies have reported data consistent with the idea that GPCRs can exists as dimers and/or higher-order oligomers [2-3] a number of issues remain unresolved. Among the most vexing of these include the proportion of any GPCR that is a dimer or oligomer at steady-state and whether this might be regulated by receptor ligands. Although a substantial literature exists on effects and lack of effects of ligands on the quaternary organisation of GPCRs [27] much of it is difficult to analyse with clarity because either there is contradictory evidence or because a single approach was used to inform the conclusions.

A group of resonance energy transfer-based techniques have become popular means to assess GPCR quaternary structure [14,28]. Herein, each of saturation BRET studies employing a pair of C-terminally eYFP- and *Renilla* luciferase-tagged forms of the OX_1 receptor and htrFRET studies employing an N-terminally SNAP-tagged form of this receptor generated data consistent with the presence of at least a proportion of this receptor as a quaternary complex over the range of expression levels that could be controlled either by altering the amount of cDNA used in transient cellular transfections or via use of an inducible expression system in cells stably harbouring forms of the OX_1 receptor. However, despite these observations it remains challenging to analyse and interpret such studies in terms of the proportion of the receptor within such complexes [29,30]. Furthermore, effects of ligands in such studies are also challenging to interpret. For example, although orexin A increased the htrFRET signal in cells expressing VSV-G-SNAP-OX_1 this was only observed at relatively low receptor construct expression, in which situation the FRET signal consistent with the presence of OX_1 dimers was also relatively low, and this was not observed following addition of OX_1 receptor antagonists. This is similar to effects reported recently by Alvarez-Curto et al. [15] for the muscarinic M_3 receptor using an equivalent approach. This may reflect that the monomer-dimer equilibrium is such that at low receptor expression levels a limited number of dimers are present, that this is increased with higher level receptor expression that would favour such interactions and that agonists promote or stabilise the quaternary complex. However, there are other possible interpretations, including that such alterations in signal may reflect movement of the receptor towards clathrin-coated pits in preparation for internalisation, for example, and hence a possible increase in potential 'by-stander' resonance energy transfer effects [21,31] rather than a specific effect on the organisation of receptor complexes. It is noteworthy that in recent times a series of studies have suggested both that GPCR-GPCR interactions may be dynamic [5,6,32] and that the extent of dimerisation may vary significantly between even closely related receptors [5]. This may be defined by the affinity of different GPCR protomers for one another and if so, implies that at equal expression densities the proportion of monomers-dimers-oligomers may be quite different for different receptors. Indeed, as ligand-induced movements of helices that have been implicated as GPCR dimer interfaces have been detected [33] then ligands might, at least in certain cases, modify these interactions. It is important, however, to consider evidence to the contrary. Whilst FRAP microscopy studies have suggested that the β_1-adrenoceptor may form a lower affinity and more transient quaternary complex than the β_2-adrenoceptor [5], saturation BRET studies [31], in which similar so called '$BRET_{50}$' values are observed for β_1-β_1-adrenoceptor interactions as for β_2-β_2-adrenoceptor interactions, have been interpreted as being consistent with these receptors having similar interaction affinities [31].

It is also worthy of note that in the absence of well characterised antibodies for many GPCRs experiments that explore organisational structure are highly reliant on molecularly modified forms of the receptors and, as in the case of a number of the studies used herein, the tags used are themselves substantial proteins. These may either generate artefacts by promoting or inhibiting receptor interactions and/or ligand-induced re-organisation. Because of some of these issues we decided additionally to address the proportion of OX_1 receptor constructs present as quaternary complexes in a range of other ways. Importantly for the BN-PAGE studies we demonstrated initially that much of the OX_1 receptor could be solubilised from cell lysates with the detergent DDM in a form that retained binding of the antagonist

[^{3}H]SB674042. Furthermore, in parallel studies employing enzyme complementation we also demonstrated that treatment with DDM did not result in non-specific aggregation of the OX_1 receptor or, indeed, in the disassembly of pre-formed dimers. To do so we employed split luciferase technology [16,34] in which two inherently non-functional fragments of *Renilla* luciferase that are able to recombine to generate a functional enzyme when brought into proximity were linked to the C-terminal tail of forms of the OX_1 receptor. Following co-transfection of these forms solubilisation with DDM resulted in soluble luciferase activity whereas, following separate transfections of each construct, solubilisation followed by mixing did not reconstitute enzyme activity. These studies are akin to the 'mixing' controls used in many co-immunoprecipitation approaches to detect authentic GPCR dimers [35,36]. These are a key set of experiments because, even although purified β_2-adrenoceptors appear able to form dimers, and indeed potential tetramers, spontaneously when reconstituted into lipid bilayers [37], extraction from baculovirus-infected insect cells with 1% DDM is sufficient to promote monomerisation of the receptor [38]. Indeed the capacity to solubilise receptors has been integral to effects to obtain atomic level structural information [39-40] and this has often resulted in monomerisation of the receptor. However, this need not intrinsically be the case. For example, atomic level structures of the CXCR4 chemokine receptor reveal a consistent homodimer configuration over a number of individual crystal forms [41] indicating that, at least in this specific case, combinations of protein engineering and the presence of a CXCR4 ligand was sufficient to preserve dimer contacts throughout solubilisation with a combination of 0.5 % DDM and 0.1% cholesteryl hemisuccinate [41]. It is also worthy of note, however, that the most notable effects of the agonist orexin A were observed when using the SNAP-tagged construct where a 20 kDa protein with enzymatic activity is placed on the extracellular face and although this does not alter the binding affinity of the antagonist [^{3}H]SB-674042 or of orexin A it might alter the orientation of the receptor in response to binding the agonist.

BN-PAGE has recently been employed to study regulation of the dimeric status of the muscarinic M_1 receptor and the effects of the MT7 toxin on this [42]. These studies indicated that the toxin either bound to and stabilised or favoured production of a dimeric form [42]. There are a range of potential issues with the use of BN-PAGE to study the quaternary structure of transmembrane proteins [22], not least in the case of GPCRs, because although this varies significantly between individual family members [43,44], detergent solubilisation often results in denaturation and aggregation [43,44]. Initially, we therefore optimised the BN-PAGE procedure by performing preliminary studies with the single transmembrane pass epidermal growth factor receptor. Following DDM solubilisation we demonstrated that this receptor migrated in BN-PAGE at a position anticipated for the monomer and that a substantial proportion of the receptor migrated at the position anticipated of a dimer following addition of EGF prior to solubilisation with DDM. Importantly, this did not reflect non-specific aggregation or some irreversible modification because addition of 1% SDS to the sample prior to resolution on BN-PAGE restored the mobility of the epidermal growth factor receptor to that anticipated for the monomer. Following DDM solubilisation VSV-G-OX_1-eYFP migrated on BN-PAGE predominantly at the position predicted for a dimer. Importantly, after treatment with 1% SDS, a substantial proportion of VSV-G-OX_1-eYFP now migrated consistent with the size of a monomer, suggesting that at least the bulk of the receptor was not aggregated and/or denatured, consistent with the ligand binding studies. Although the extent of this effect varied somewhat between experiments, a number of key points

should be noted. Firstly, this occurred across a substantial range of expression levels as controlled by the extent of induction of the receptor constructs. Secondly, this effect of SDS was more pronounced when studying VSV-G-OX_1-eYFP than the VSV-G-SNAP-OX_1 construct. We do not have a ready explanation for this but the SNAP-tag is a recently developed means of introducing covalently linked labels into proteins [45,46] and rather little is known about its specific properties and any undesirable effects it might have in such studies. Thirdly, it was at least conceptually possible that much of the OX_1 receptor constructs migrating at a position consistent with an OX_1 receptor dimer on BN-PAGE might reflect a monomer of the OX_1 receptor in association with an unidentified GPCR-interacting protein. To address this we generated cells expressing HA-OX_1-eYFP constitutively but also able to express VSV-G-OX_1-eYFP on demand. Following induction of VSV-G-OX_1-eYFP, anti-VSV-G immunoprecipitation, elution and subsequent BN-PAGE, immunoblotting demonstrated the anti-HA immunoreactivity to migrate in the position of the predicted OX_1-eYFP dimer. This must contain VSV-G-OX_1-eYFP as well as HA-OX_1-eYFP and pre-addition of 1% SDS resulted in a large proportion of HA-OX_1-eYFP now migrating in the position expected for this monomer. This provides clear support that the protein detected with lower mobility was a HA-OX_1-eYFP + VSV-G-OX_1-eYFP dimer.

Not all of the OX_1 receptor construct that migrated in BN-PAGE at the position consistent with a receptor dimer was disaggregated by treatment with 1% SDS prior to resolution. It is certainly possible that some of this represents aggregated protein as it is well established that many GPCRs are not highly stable after detergent extraction [43-44]. However, it should also be noted that even in SDS-PAGE a substantial fraction of many GPCRs migrate with apparent mass consistent with them behaving as an SDS-resistant dimer [47,48] and, indeed, in many studies this characteristic has been used to support other evidence of GPCR quaternary structure.

Interestingly, although the addition of orexin A to samples expressing VSV-G-OX_1-eYFP had little noticeable effect on the mobility of the construct in BN-PAGE the agonist produced a marked alteration in pattern when using VSV-G-SNAP-OX_1. Now, a substantial proportion of the receptor migrated at a size consistent with production of a higher-order oligomer. Moreover, this was reversed entirely by addition of 1% SDS prior to resolution on BN-PAGE. This is at least consistent with agonist-mediated production of a large, reversible, quaternary complex. However, as this was not replicated when studying VSV-G-OX_1-eYFP it may indicate that the SNAP-tag is at least in part responsible for the observations. As SNAP-tagged receptors have not been studied in this manner previously it will be important for such possible effects to be monitored in future studies, not least because this emerging technology is becoming a popular approach [14,30]. As well as the effects of orexin A, addition of OX_1 receptor antagonists increased the proportion of OX_1 receptor constructs migrating in BN-PAGE in a position consistent with a receptor monomer and this was the case for both VSV-G-SNAP-OX_1 and VSV-G-OX_1-eYFP. This may indeed indicate that binding of antagonists reduces the affinity of OX_1 protomers for each other and modulates the equilibrium between receptor monomers and dimers. A second possibility, however, as receptor ligands are known to stabilize GPCR structure [49], is that the antagonists are limiting receptor denaturation. It was clear that this effect of OX_1 receptor antagonists was concentration-dependent and that the EC_{50} for these effects was similar to the binding affinity of the ligands. Recent studies have suggested that rather than promoting monomerisation, the M_1 muscarinic receptor selective antagonist pirenzipine can promote dimerisation [50] but there is no

inherent reason to assume that the effects of ligands on such complexes will be consistent across family members and meaningful insight will only emerge with the publication of further studies. Although we did perform a series of densitometry studies these were designed to provide information on the concentration of antagonist ligands that produced half-maximal effects in altering the apparent dimer-monomer equilibrium rather than being designed to provide absolute values for this ratio. Densitometry is susceptible to film saturation artefacts and limited reproducibility between experiments. As such we have avoided attempting to over-interpret these studies in quantitative terms.

These studies provide novel insight into the proportion of orexin OX_1 receptors that exist as dimers and hint at a general means to assess this for GPCRs that are either inherently sufficiently stable to withstand denaturation upon solubilisation or have been engineered to enhance such stability [43,44].

ACKNOWLEDGEMENTS

These studies were supported by the Medical Research Council (grant G0900050).
We thank Sarah Cummings, University of Glasgow for assistance with a series of preliminary experiments.

REFERENCES

1 Chabre, M., and le Maire, M. (2005) Monomeric G-protein-coupled receptor as a functional unit. Biochemistry **44**, 9395-9403

2 Milligan, G. (2008) A day in the life of a G protein-coupled receptor: the contribution to function of G protein-coupled receptor dimerization. Br. J. Pharmacol. **153,** Suppl 1:S216-229

3 Milligan, G. (2007) G protein-coupled receptor dimerisation: molecular basis and relevance to function. Biochim. Biophys. Acta **1768**, 825-835

4 Pin, J.P., Kniazeff, J., Liu, J., Binet, V., Goudet, C., Rondard, P., and Prézeau, L. (2005) Allosteric functioning of dimeric class C G-protein-coupled receptors. FEBS J. **272**, 2947-2955

5 Dorsch, S., Klotz, K.N., Engelhardt, S., Lohse, M.J., and Bünemann, M. (2009) Analysis of receptor oligomerization by FRAP microscopy. Nat. Methods **6**, 225-230

6 Hern, J.A., Baig, A.H., Mashanov, G.I., Birdsall, B., Corrie, J.E., Lazareno, S., Molloy, J.E., and Birdsall, N.J. (2010) Formation and dissociation of M1 muscarinic receptor dimers seen by total internal reflection fluorescence imaging of single molecules. Proc. Natl. Acad. Sci. U S A **107**, 2693-2698

7 Sakurai, T. (2005) Reverse pharmacology of orexin: from an orphan GPCR to integrative physiology. Regul. Pept. **126**, 3-10

8 Bingham, M.J., Cai, J., and Deehan, M.R. (2006) Eating, sleeping and rewarding: orexin receptors and their antagonists. Curr. Opin. Drug. Discov. Devel. **9**, 551-559

9 Kroeger, D., and de Lecea, L. (2009) The hypocretins and their role in narcolepsy. CNS Neurol. Disord. Drug Targets **8**, 271-280

10 Neubauer, D.N. (2010) Almorexant, a dual orexin receptor antagonist for the treatment of insomnia. Curr. Opin. Investig. Drugs **11**, 101-110

11 Ellis, J., Pediani, J.D., Canals, M., Milasta, S., and Milligan, G. (2006) Orexin-1 receptor-cannabinoid CB1 receptor heterodimerization results in both ligand-dependent and -independent coordinated alterations of receptor localization and function. J. Biol. Chem. **281**, 38812-38824

12 Swamy, M., Siegers, G.M., Minguet, S., Wollscheid, B., and Schamel, W.W. (2006) Blue native polyacrylamide gel electrophoresis (BN-PAGE) for the identification and analysis of multiprotein complexes. Sci STKE. **345**, pl4.

13 Reisinger, V., and Eichacker, L.A. (2006) Analysis of membrane protein complexes by blue native PAGE. Proteomics **6** Suppl 2, 6-15

14 Alvarez-Curto, E., Pediani, J.D., and Milligan, G. (2010) Applications of fluorescence and bioluminescence resonance energy transfer to drug discovery at G protein coupled receptors. Anal. Bioanal. Chem. **398**, 167-180

15 Alvarez-Curto, E., Ward, R.J., Pediani, J.D., and Milligan G. (2010) Ligand regulation of the quaternary organization of cell surface M3 muscarinic acetylcholine receptors analyzed by fluorescence resonance energy transfer (FRET) imaging and homogeneous time-resolved FRET. J. Biol. Chem. **285**, 23318-23330

16 Eglen, R.M. (2002) Enzyme fragment complementation: a flexible high throughput screening assay technology. Assay Drug Dev. Technol. **1**, 97-104

17 De, A., Ray, P., Loening, A.M., and Gambhir, S.S. (2009) BRET3: a red-shifted bioluminescence resonance energy transfer (BRET)-based integrated platform for

imaging protein-protein interactions from single live cells and living animals. FASEB J. **23**, 2702-2709

18 Ward, R.J., Pediani, J.D., and Milligan, G. (2011) Ligand-induced internalization of the orexin OX_1 and cannabinoid CB_1 receptors assessed via N-terminal SNAP and CLIP-tagging. *Br. J. Pharmacol*. **162**, 1439-1452.

19 Carrillo, J.J., López-Gimenez, J.F., and Milligan, G. (2004) Multiple interactions between transmembrane helices generate the oligomeric alpha1b-adrenoceptor. Mol. Pharmacol. **66,** 1123-1137

20 Milasta, S., Evans, N.A., Ormiston, L., Wilson, S., Lefkowitz, R.J., and Milligan, G. (2005) The sustainability of interactions between the orexin-1 receptor and beta-arrestin-2 is defined by a single C-terminal cluster of hydroxy amino acids and modulates the kinetics of ERK MAPK regulation. Biochem. J. **387**, 573-584.

21 Bouvier, M., Heveker, N., Jockers, R., Marullo, S., and Milligan, G. (2007) BRET analysis of GPCR oligomerization: newer does not mean better. Nat. Methods **4**, 3-4

22 Tate, C.G. (2010) Practical considerations of membrane protein instability during purification and crystallisation. Methods Mol. Biol. **601**, 187-203

23 Chung, I., Akita, R., Vandlen, R., Toomre, D., Schlessinger, J., and Mellman, I. (2010) Spatial control of EGF receptor activation by reversible dimerization on living cells. Nature **464**, 783-787

24 Kawashima N., Nakayama K., Itoh K., Itoh T., Ishikawa M., Biju V. (2010) Reversible dimerization of EGFR revealed by single-molecule fluorescence imaging using quantum dots. Chemistry **16**, 1186-1192

25 Smith, N.J., Stoddart, L.A., Devine, N.M., Jenkins, L., and Milligan G. (2009) The action and mode of binding of thiazolidinedione ligands at free fatty acid receptor 1. J. Biol. Chem. **284**, 17527-17539.

26 Maurel, D., Comps-Agrar, L., Brock, C., Rives, M.L., Bourrier, E., Ayoub, M.A., Bazin, H., Tinel, N., Durroux, T., Prézeau, L., Trinquet, E., and Pin, J.P. (2008) Cell-surface protein-protein interaction analysis with time-resolved FRET and snap-tag technologies: application to GPCR oligomerization. Nat. Methods **5**, 561-567

27 Saenz del Burgo, L. and Milligan, G. (2011) In: 'G protein-coupled receptors: from structure to function'. Eds Giraldo, J. and Pin, J.P. RSC Drug Discovery Series, Royal Society of Chemistry Publishing pp111-152.

28 Gandía, J., Lluís, C., Ferré, S., Franco, R., and Ciruela, F. (2008) Light resonance energy transfer-based methods in the study of G protein-coupled receptor oligomerization. Bioessays **30**, 82-89.

29 Pisterzi, L.F., Jansma, D.B., Georgiou, J., Woodside, M.J., Chou, J.T., Angers, S., Raicu, V., and Wells, J.W. (2010) Oligomeric size of the m2 muscarinic receptor in live cells as determined by quantitative fluorescence resonance energy transfer. J. Biol. Chem. **285**, 16723-16738

30 Doumazane, E., Scholler, P., Zwier, J.M., Trinquet, E., Rondard, P., and Pin, J.P. (2011) A new approach to analyze cell surface protein complexes reveals specific heterodimeric metabotropic glutamate receptors. FASEB J. **25**, 66-77

31 Mercier, J.F., Salahpour, A., Angers, S., Breit, A., and Bouvier, M. (2002) Quantitative assessment of beta 1- and beta 2-adrenergic receptor homo- and heterodimerization by bioluminescence resonance energy transfer. J. Biol. Chem. **277**, 44925-44931

32 Fonseca, J.M., and Lambert, N.A. (2009) Instability of a class a G protein-coupled receptor oligomer interface. Mol. Pharmacol. **75**, 1296-1299

33 Han, Y., Moreira, I.S., Urizar, E., Weinstein, H., and Javitch, J.A. (2009) Allosteric communication between protomers of dopamine class A GPCR dimers modulates activation. Nat. Chem. Biol. **5**, 688-695.

34 Kato, N., Jones, J. (2010) The split luciferase complementation assay. Methods Mol. Biol. **655**, 359-376

35 McVey, M., Ramsay, D., Kellett, E., Rees, S., Wilson, S., Pope, A.J., and Milligan, G. (2001) Monitoring receptor oligomerization using time-resolved fluorescence resonance energy transfer and bioluminescence resonance energy transfer. The human delta -opioid receptor displays constitutive oligomerization at the cell surface, which is not regulated by receptor occupancy. J. Biol. Chem. **276**, 14092-14099

36 Jordan, B.A., Trapaidze, N., Gomes, I., Nivarthi, R., and Devi, L.A. (2001) Oligomerization of opioid receptors with beta 2-adrenergic receptors: a role in trafficking and mitogen-activated protein kinase activation. Proc. Natl. Acad. Sci. U S A **98**, 343-348

37 Fung, J.J., Deupi, X., Pardo, L., Yao, X.J., Velez-Ruiz, G.A., Devree, B.T., Sunahara, R.K., and Kobilka, B.K. (2009) Ligand-regulated oligomerization of beta(2)-adrenoceptors in a model lipid bilayer. EMBO J. **28**, 3315-3328

38 Whorton, M.R., Bokoch, M.P., Rasmussen, S.G., Huang, B., Zare, R.N., Kobilka, B., and Sunahara, R.K. (2007) A monomeric G protein-coupled receptor isolated in a high-density lipoprotein particle efficiently activates its G protein. Proc. Natl. Acad. Sci. U S A **104**, 7682-7687

39 Rosenbaum, D.M., Rasmussen, S.G., and Kobilka, B.K. (2009) The structure and function of G-protein-coupled receptors. Nature **459**, 356-363

40 Cherezov, V., Abola, E., and Stevens, R.C. (2010) Recent progress in the structure determination of GPCRs, a membrane protein family with high potential as pharmaceutical targets. Methods Mol. Biol. **654**, 141-168

41 Wu, B., Chien, E.Y., Mol, C.D., Fenalti, G., Liu, W., Katritch, V., Abagyan, R., Brooun, A., Wells, P., Bi, F.C., Hamel, D.J., Kuhn, P., Handel, T.M., Cherezov, V., and Stevens, R.C. (2010) Structures of the CXCR4 chemokine GPCR with small-molecule and cyclic peptide antagonists. Science **330**, 1066-1071

42 Marquer, C., Fruchart-Gaillard, C., Mourier, G., Grandjean, O., Girard, E., le Maire, M., Brown, S., Servent, D. (2010) Influence of MT7 toxin on the oligomerization state of the M1 muscarinic receptor. Biol. Cell **102**, 409-420

43 Robertson, N., Jazayeri, A., Errey, J., Baig, A., Hurrell, E., Zhukov, A., Langmead, C.J., Weir, M., and Marshall, F.H. (2011) The properties of thermostabilised G protein-coupled receptors (StaRs) and their use in drug discovery. Neuropharmacology **60**, 36-44

44 Magnani, F., Shibata, Y., Serrano-Vega, M.J., and Tate, C.G. (2008) Co-evolving stability and conformational homogeneity of the human adenosine A2a receptor. Proc. Natl. Acad. Sci. U S A **105**, 10744-10749

45 Ciruela, F., Vilardaga, J.P., and Fernández-Dueñas, V. (2010) Lighting up multiprotein complexes: lessons from GPCR oligomerization. Trends Biotechnol. **28**, 407-415

46 Brun, M.A., Tan, K.T., Nakata, E., Hinner, M.J., Johnsson, K. (2009) Semisynthetic fluorescent sensor proteins based on self-labeling protein tags. J. Am. Chem. Soc. **131**, 5873-5884

47 Hebert, T.E., Moffett, S., Morello, J-P., Loisel, T.P., Bichet, D.G., Barret, C., and Bouvier M. (1996) A peptide derived from a beta2-adrenergic receptor transmembrane domain inhibits both receptor dimerization and activation. J. Biol. Chem. **271**, 16384-16392

48 Sanchez-Laorden, B.L., Sanchez-Mas, J., Martinez-Alonso, E., Martinez-Menarguez, J.A., Garcia-Borron, J.C., and Jimenez-Cervantes, C. (2006) Dimerization of the human melanocortin 1 receptor: functional consequences and dominant-negative effects. J. Invest. Dermatol. **126**, 172-181

49 Zeng, F.Y., McLean, A.J., Milligan, G., Lerner, M., Chalmers, D.T., and Behan, D.P. (2003) Ligand specific up-regulation of a Renilla reniformis luciferase-tagged, structurally unstable muscarinic M3 chimeric G protein-coupled receptor. Mol. Pharmacol. **64**, 1474-1484

50 Ilien, B., Glasser, N., Clamme, J.P., Didier, P., Piemont, E., Chinnappan, R., Daval, S.B., Galzi, J.L., and Mely, Y. (2009) Pirenzepine promotes the dimerization of muscarinic M1 receptors through a three-step binding process. J. Biol. Chem. **284**, 19533-19543

FIGURE LEGENDS

Figure 1 BRET assays indicate that VSV-G-OX_1-eYFP forms dimers/oligomers

VSV-G-OX_1-eYFP and VSV-G-OX_1-Rluc8 were transiently co-expressed in various ratios in HEK293T cells. (**A**) Following addition of coelenterazine-h BRET was measured. (**B**) In equivalent studies VSV-G-OX_1-eYFP was co-expressed with α_{1b}-adrenoceptor-Rluc8 or VSV-G-OX_1-Rluc8 was co-expressed with α_{1b}-adrenoceptor-eYFP. BRET was recorded and signals at eYFP/Rluc8 = 0.1 are displayed. Data are representative of three independent experiments.

Figure 2 DDM solubilises a high proportion of VSV-G-OX_1-eYFP

Flp-In™ T-REx™ 293 cells harbouring VSV-G-OX_1-eYFP were treated with (dox) or without (no dox) doxycycline for 24 h. Cell lysates were incubated with 5nM [^{3}H]SB-674042 +/- 3 μM SB-408124 to define total and non-specific binding. Samples were then treated as in Experimental. 100% specific binding of [^{3}H]SB-674042 corresponds to 3.7 +/- 0.08 pmol.mg protein^{-1}. 4 other experiments produced similar results.

Figure 3 BN-PAGE shows VSV-G-OX_1-eYFP migrates consistent with being predominantly a dimer

BN-PAGE was used to resolve proteins extracted from Flp-In™ T-REx™ 293 cells able to express VSV-G-OX_1-eYFP on demand with 0.5% DDM. (**A**) Samples were transferred to a PVDF membrane and immunoblotted to detect the VSV-G tag, with two different exposures of the same samples shown. The migration of marker proteins is shown in the left hand lane. (**B**) Prior to separation on BN-PAGE samples from cells induced to express VSV-G-OX_1-eYFP for 24 h had varying concentrations of SDS added. Equivalent anti-VSV-G immunoreactivity is shown. (**C**) Equivalent BN-PAGE experiments were performed on cells treated with or without epidermal growth factor and with and without 1% SDS before separation. The migration of the epidermal growth factor receptor was then detected with a polyclonal anti-epidermal growth factor receptor antiserum following transfer of samples to a PVDF membrane. Each element of this Figure was reproduce in at least 3 independent experiments.

Figure 4 Luciferase enzyme complementation assays demonstrate that DDM solubilisation does not generate artificial OX_1 receptor dimers

HEK293T cells were transiently transfected to express either VSV-G-OX_1-Rluc8N or VSV-G-OX_1-Rluc8C (left hand side) or were transfected to co-express this pairing (right hand side). Following solubilisation using 0.5% DDM and sample preparation *Renilla* luciferase activity was measured.

Figure 5 VSV-G-OX_1-eYFP is predominantly a dimer at a range of expression levels

Flp-In™ T-REx™ 293 cells harbouring VSV-G-OX_1-eYFP at the Flp-In™ locus were either not induced (0 h) or induced to express this polypeptide by treatment with doxycycline for varying times. (**A**) Cell lysate samples were used to measure VSV-G-OX_1-eYFP expression based on the specific binding of [^{3}H]SB674042. (**B**) Following 0.5% DDM solubilisation samples were resolved by BN-PAGE. In both cases parental Flp-In™ T-REx™ 293 (Flp-In) cells provided an extra 'no expression' control. In (**B**) samples of cells induced with doxycycline for 24 h were treated with buffer or 1% SDS before electrophoresis on a Blue-Native gel. Quantification, based on densitometry, of the apparent monomer and dimer levels are shown in (**C**). Each element of the Figure was derived from 3 independent experiments.

Figure 6 OX_1 antagonists but not orexin A modify mobility of VSV-G-OX_1-eYFP on BN-PAGE

Samples were prepared for BN-PAGE from un-induced (-dox) and 24 h doxycycline-treated Flp-In™ T-REx™ 293 cells harbouring VSV-G-OX_1-eYFP. Prior to solubilisation with 0.5% DDM cells were treated with vehicle or with orexin A (10^{-6}M or 10^{-7}M), or with the OX_1 antagonists SB334867 or SB408124 (10^{-6}M) for 40 mins. Samples were subsequently resolved by BN-PAGE and immunoblotted with anti-VSV-G. Experiments akin to those of (**A**) were performed (**B**) and quantified (**C**) after addition of varying concentrations of SB334867. A further set of experiments produced similar results.

Figure 7 VSV-G-OX_1 behaves similarly to VSV-G-OX_1-eYFP on BN-PAGE

Panel **A,** samples were prepared for BN-PAGE from un-induced (-dox) and 24 h doxycycline-induced Flp-In™ T-REx™ 293 cells harbouring VSV-G-OX_1. Prior to solubilisation with 0.5% DDM cells were treated with vehicle or with orexin A (10^{-6}M), or with the OX_1 antagonist SB334867 (10^{-6}M) for 40 min, A VSV-G-OX_1-eYFP sample is also shown for comparison. Samples were subsequently resolved by BN-PAGE and immunoblotted with anti-VSV-G. As in **Figure 6** equivalent experiments to those in (**A**) were performed using varying concentrations of SB334867 (**B**) and quantified (**C**). 4 separate experiments were performed with similar results.

Figure 8 Co-immunoprecipitation studies show the 180kDa species is an OX_1-eYFP dimer

Flp-In™ T-REx™ 293 cells in which VSV-G-OX_1-eYFP was located at the inducible locus whilst HA-OX_1-eYFP was expressed constitutively were untreated or treated with doxycycline. Lysates of these cells were prepared. Following extraction of such lysates with 0.5% DDM and clearance by centrifugation, immunoprecipitation was performed with anti-VSV-G agarose beads. These were subsequently eluted with VSV-G peptide. Samples of the lysates and eluates of the immunoprecipitates were treated with or without 1% SDS, resolved by BN-PAGE and immunoblotted to detect either the HA- (**A**) or VSV-G epitope (**B**) tags. The longer exposure time in (**A**) is included to indicate that no monomeric HA-OX_1-eYFP could be detected without

treatment of the sample with SDS. Similar results were produced in three further experiments.

Figure 9 VSV-G-OX_1-eYFP and VSV-G-SNAP-OX_1 receptor behave similarly on BN-PAGE and SDS-PAGE

Lysates from Flp-In™ T-REx™ 293 cells induced to express VSV-G-OX_1-eYFP or VSV-G-SNAP-OX_1 were (**A**) resolved by SDS-PAGE or (**B**) BN-PAGE and immunoblotted to detect the VSV-G tag. Expression controls were provided by uninduced (- DOX) Flp-In™ T-REx™ 293 cells harbouring VSV-G-OX_1-eYFP. (**C**). The effects of varying concentration of SDS on the mobility of VSV-G-SNAP-OX_1 in BN-PAGE was assessed. Experiments were repeated on more than 3 other sample sets.

Figure 10 Regulation of VSV-G-SNAP-OX_1 receptor migration in BN-PAGE by receptor ligands

Experiments akin to those of Figure 7 were performed following treatment of cells induced to express either low (1 $ng.ml^{-1}$ dox) or higher (100 $ng.ml^{-1}$ dox) VSV-G-SNAP-OX_1 with either orexin A, SB334867 or SB408124 for 40 min. A second independent experiment produced similar results.

Figure 11 At low expression levels cell surface VSV-G-SNAP-OX_1 dimer/oligomer htrFRET signals are enhanced by orexin A

htrFRET signals assessed as 665/620 nm ratio were measured over time in Flp-In™ T-REx™ 293 cells not induced (**A**) and induced to express VSV-G-SNAP-OX_1 by treatment for 24 h with differing concentrations of doxycycline (**B-D**). In cells expressing the construct htrFRET signals were monitored over a 60 min period. These were essentially unaltered by the presence of the OX_1 antagonists SB334867 and SB408124 (10^{-6}M) but at low expression levels (**B**) increased and subsequently maintained in the presence of orexin A (10^{-6}M). The data are representative sets taken from 3 independent experiments.

Biochemical Journal Immediate Publication. Published on 19 Jul 2011 as manuscript BJ20110230

Figure 1

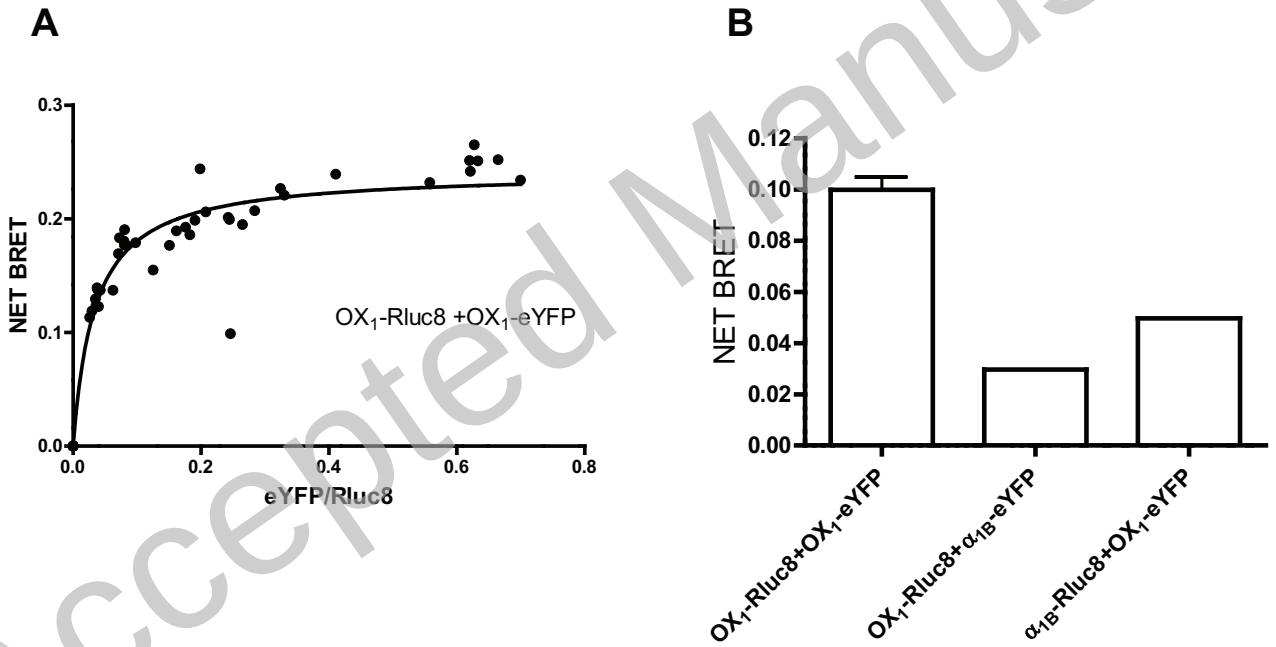

Biochemical Journal Immediate Publication. Published on 19 Jul 2011 as manuscript BJ20110230

Figure 2

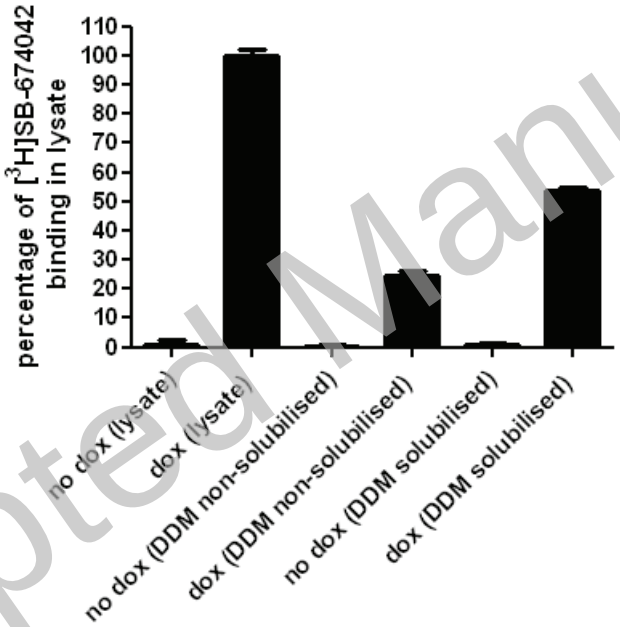

Biochemical Journal Immediate Publication. Published on 19 Jul 2011 as manuscript BJ20110230

Figure 3

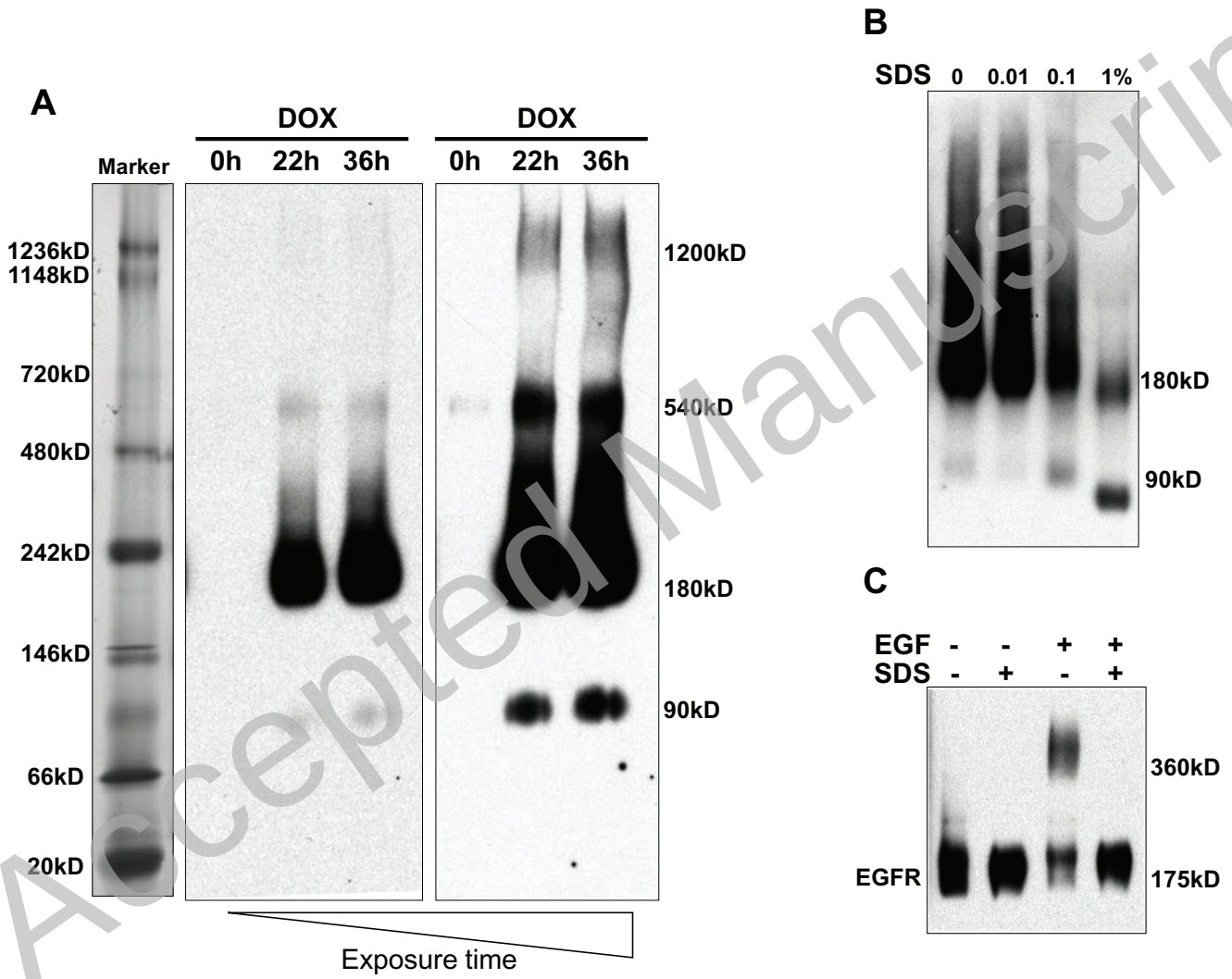

Biochemical Journal Immediate Publication. Published on 19 Jul 2011 as manuscript BJ20110230

Figure 4

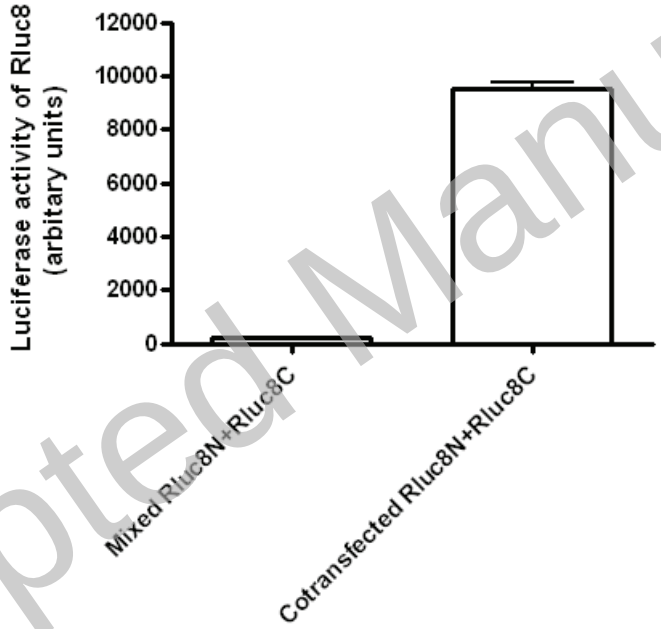

Biochemical Journal Immediate Publication. Published on 19 Jul 2011 as manuscript BJ20110230

Figure 5

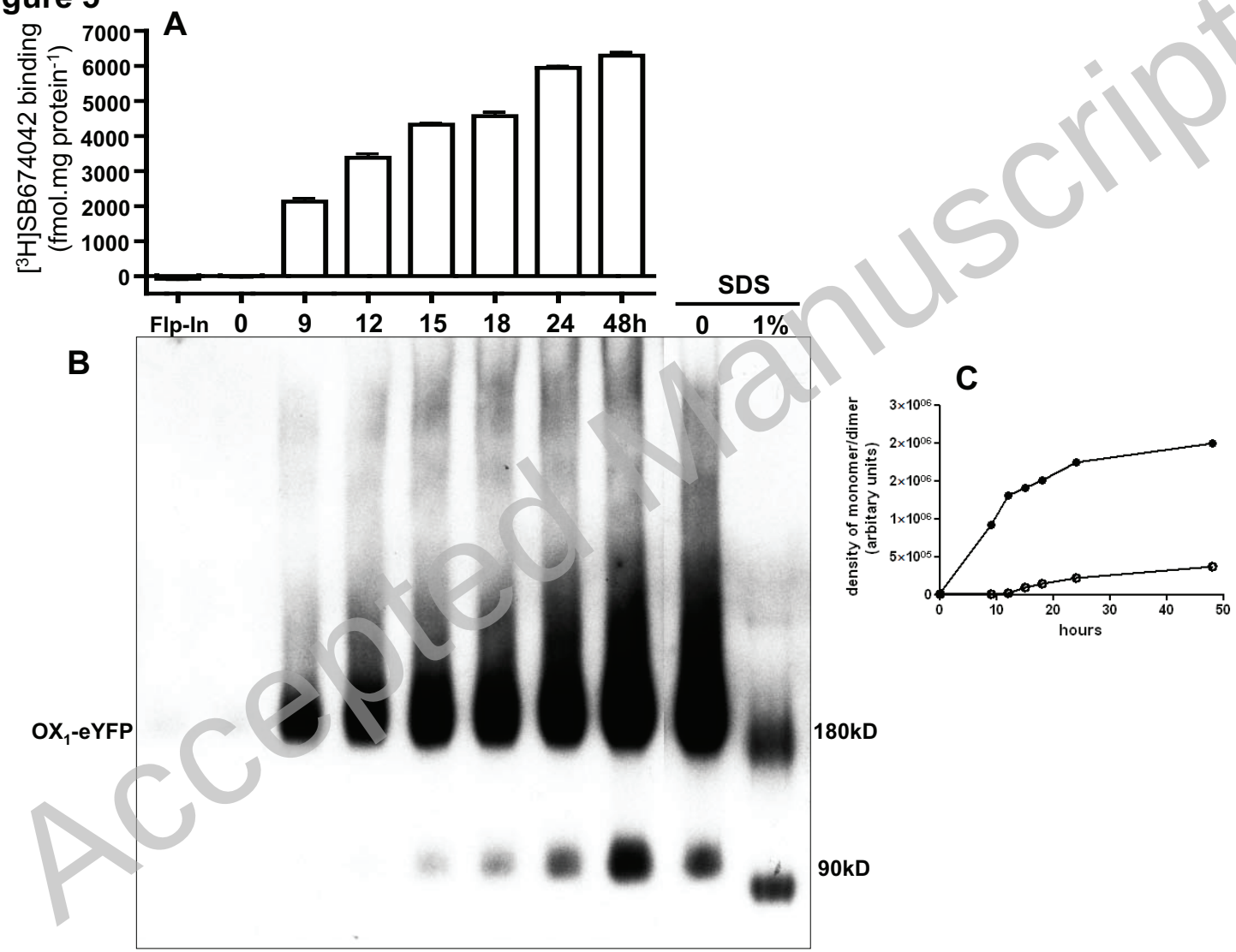

Biochemical Journal Immediate Publication. Published on 19 Jul 2011 as manuscript BJ20110230

Figure 6

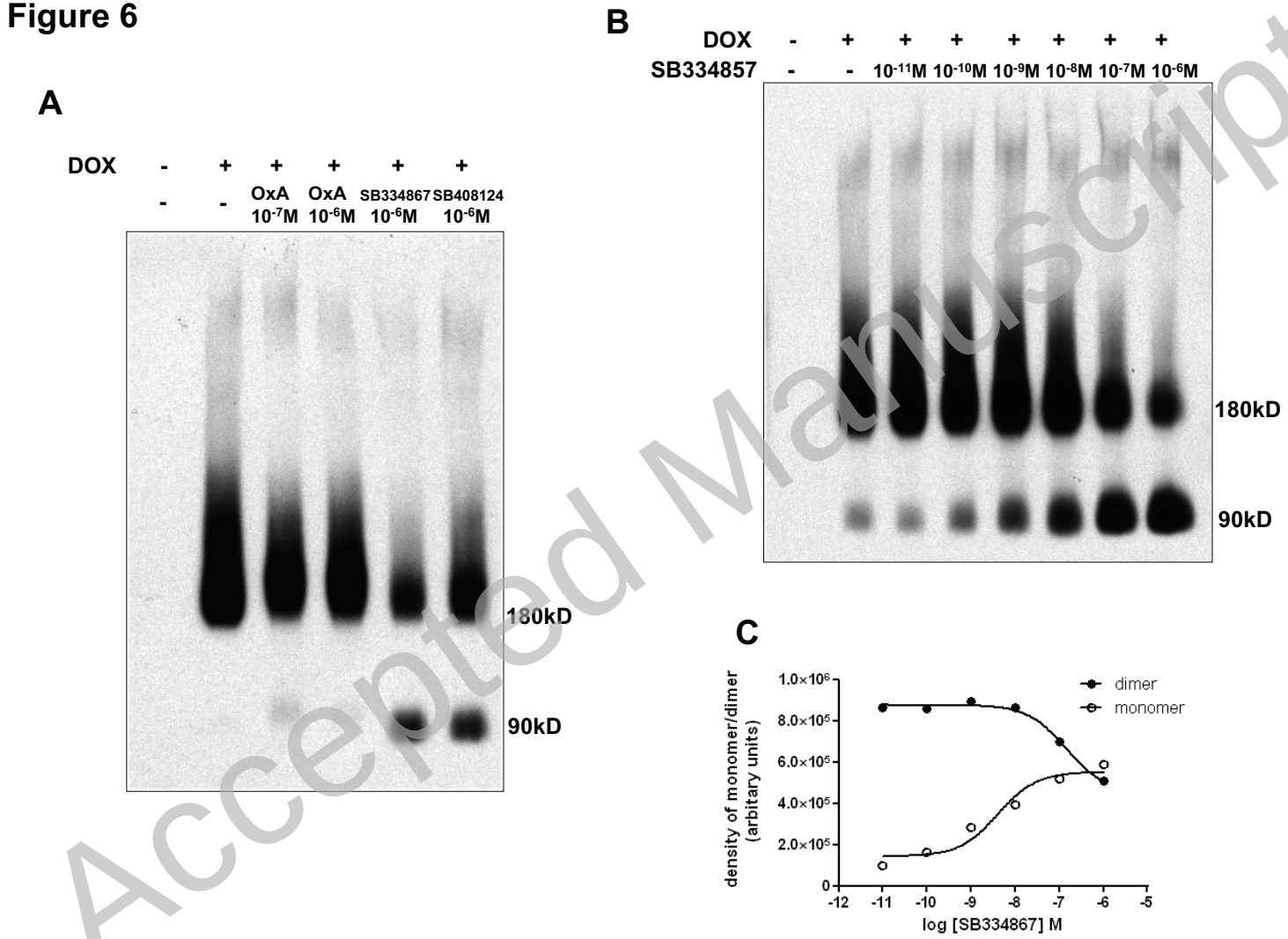

Biochemical Journal Immediate Publication. Published on 19 Jul 2011 as manuscript BJ20110230

Figure 7

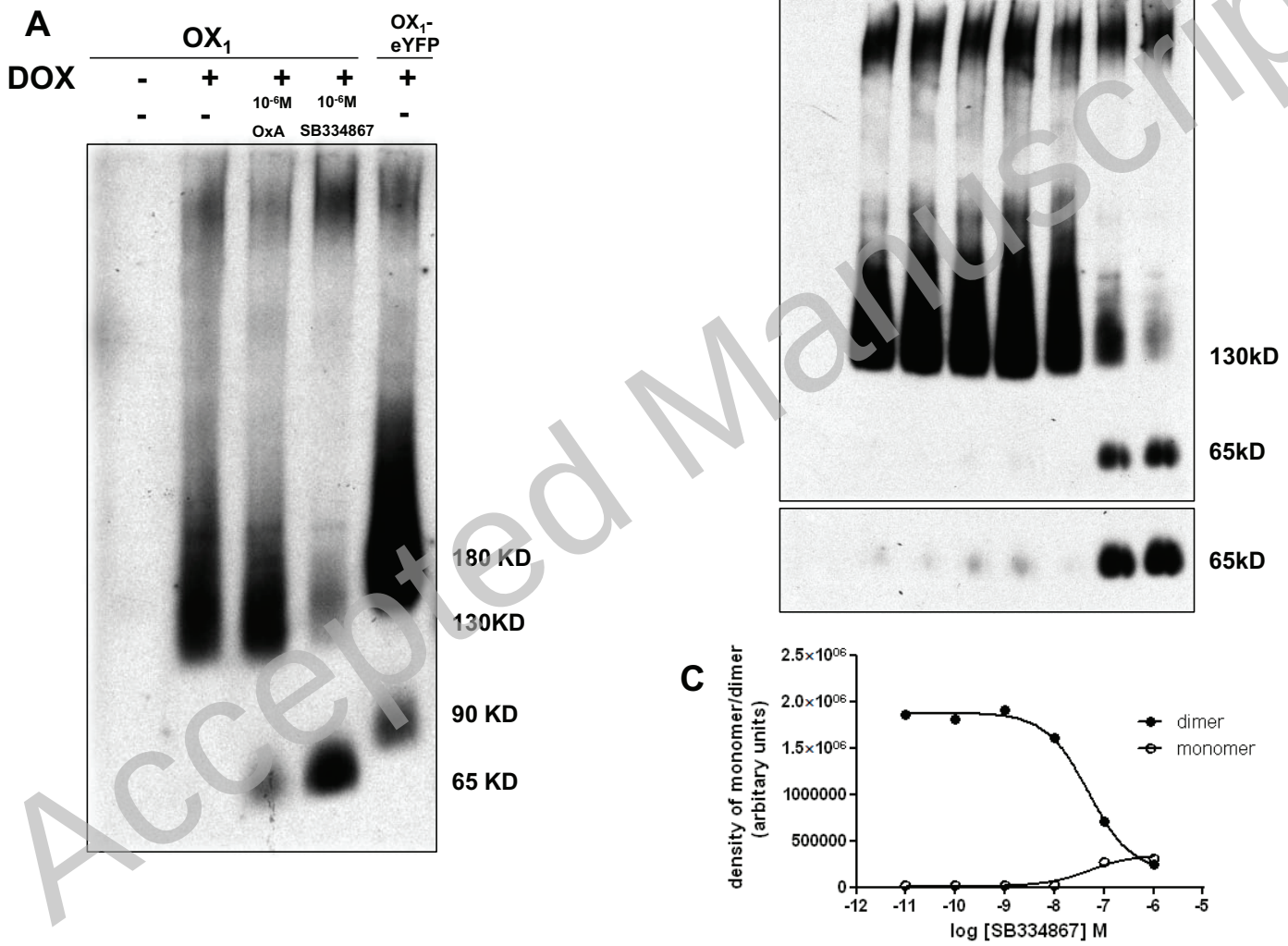

Biochemical Journal Immediate Publication. Published on 19 Jul 2011 as manuscript BJ20110230

Figure 8

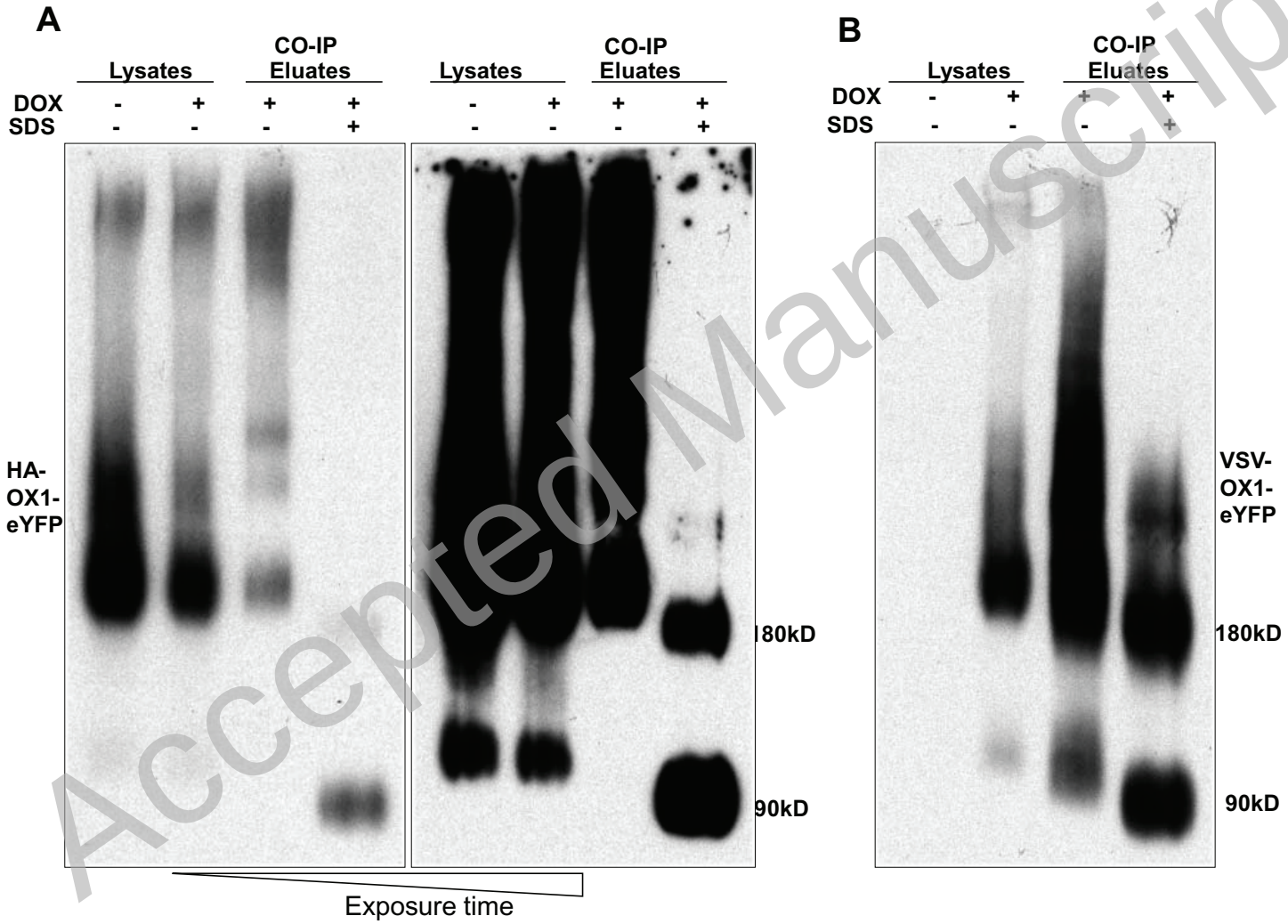

Biochemical Journal Immediate Publication. Published on 19 Jul 2011 as manuscript BJ20110230

Figure 9

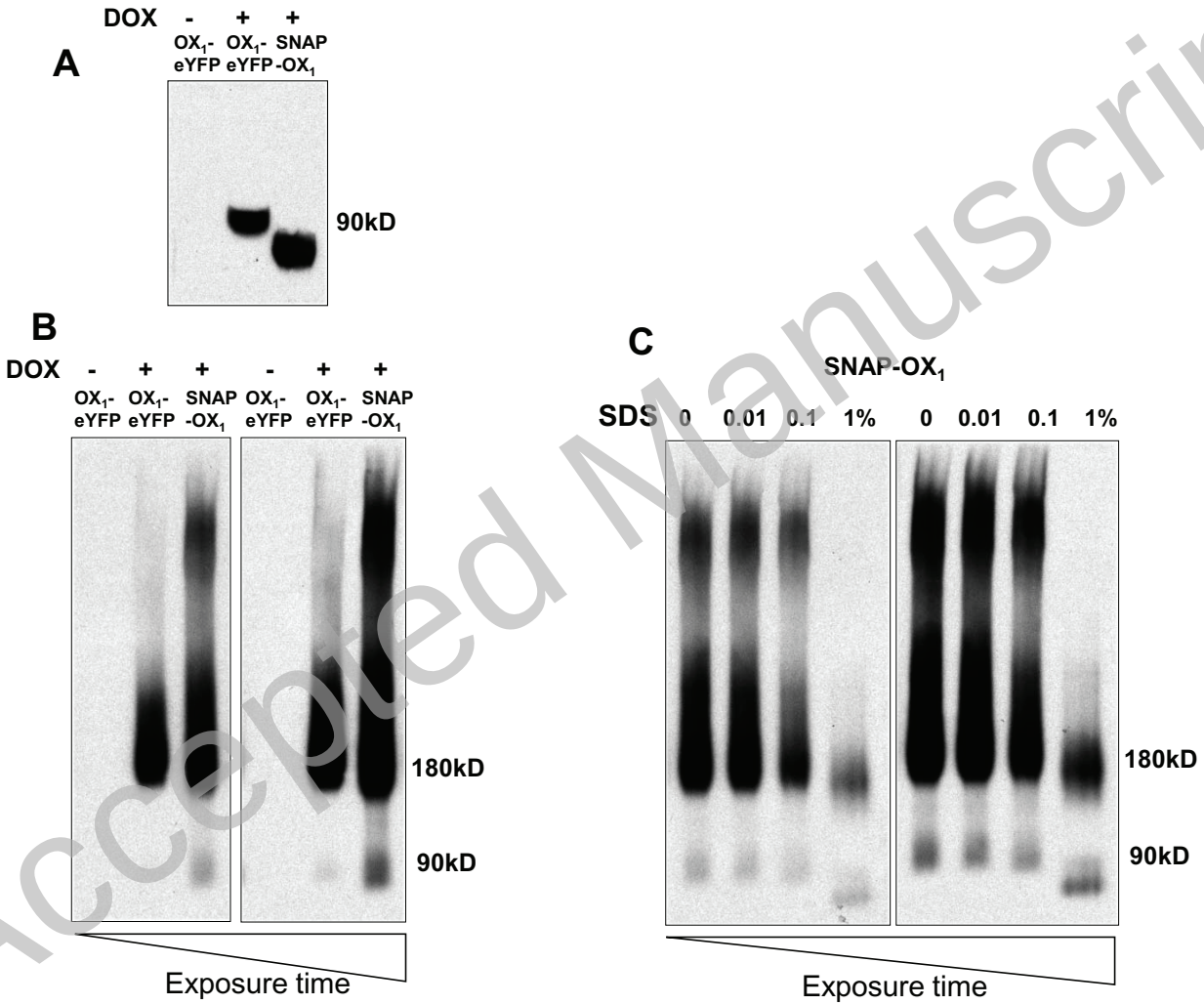

Biochemical Journal Immediate Publication. Published on 19 Jul 2011 as manuscript BJ20110230

Figure 10

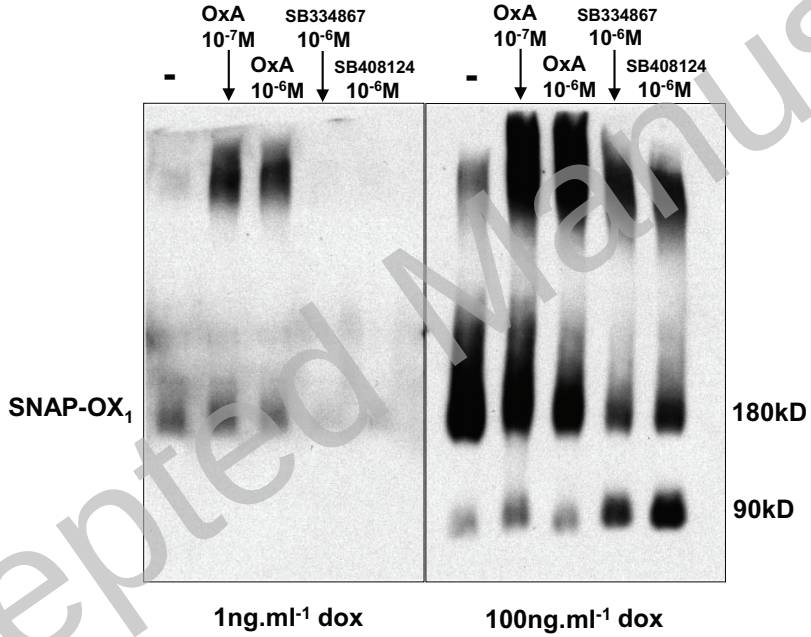

Biochemical Journal Immediate Publication. Published on 19 Jul 2011 as manuscript BJ20110230

Figure 11